Brief Report

Cloning, purification, crystallization and X-ray crystallographic analysis of the periplasmic sensing domain of *Pseudomonas fluorescens* chemotactic transducer of amino acids type A (CtaA)

Abu Iftiaf Md Salah Ud-Din[1], Anna Roujeinikova[1,2,*]

[1] *Infection and Immunity Program, Monash Biomedicine Discovery Institute, Australia; Department of Microbiology, Monash University, Clayton, Victoria, Australia;*

[2] *Infection and Immunity Program, Monash Biomedicine Discovery Institute, Australia; Department of Biochemistry and Molecular Biology, Monash University, Clayton, Victoria, Australia.*

Summary   **Chemotaxis towards nutrients plays a crucial role in root colonization by *Pseudomonas fluorescens*. The *P. fluorescens* chemotactic transducer of amino acids type A (CtaA) mediates movement towards amino acids present in root exudates. In this study, the periplasmic sensory domain of CtaA has been crystallized by the hanging-drop vapor diffusion method using ammonium sulfate as a precipitating agent. A complete data set was collected to 1.9 Å resolution using cryocooling conditions and synchrotron radiation. The crystals belong to space group *I*222 or *I*$2_1 2_1 2_1$, with unit-cell parameters a = 67.2, b = 76.0, c = 113.3 Å. This is an important step towards elucidation of the structural basis of how CtaA recognizes its signal molecules and transduces the signal across the membrane.**

Keywords: Bacterial chemotaxis, chemoreceptor, sensing domain, symbiosis

1. Introduction

Pseudomonas fluorescens belongs to the plant growth promoting rhizobacteria (PGPR), the group of bacteria that provide nutrients for plant growth, induce systemic resistance against diseases, and help plants to tolerate abiotic and biotic stress (*1-3*). Some strains of *P. fluorescens* exert beneficial effects on plants by inhibiting the growth, or actions of, phytopathogenic microorganisms such as *Pythium ultimum*, *Gaeumannomyces graminis* and *Fusarium oxysporum* (*2*). They produce different types of secondary metabolites including antibiotics (mupirocin, pyrrolnitrin, pyoluteorin and 2,4-diacetylphloroglucinol), siderophores (pyocheline and pyoverdine) and hydrogen

Address correspondence to:
Dr. Anna Roujeinikova, Infection and Immunity Program, Monash Biomedicine Discovery Institute, Australia; Department of Microbiology, Monash University, Clayton, Victoria 3800, Australia; Department of Biochemistry and Molecular Biology, Monash University, Clayton, Victoria 3800, Australia.
E-mail: anna.roujeinikova@monash.edu

cyanide, that prevent plant seeds and roots from fungal infection (*4-6*). Furthermore, some strains of *P. fluorescens* can degrade pollutants including styrene, trinitrotoluene and polycyclic aromatic hydrocarbons (*7-9*). In humans, *P. fluorescens* is part of the gut microflora (*10*). It can cause bacteraemia in immunocompromised patients (*11*).

Root colonization by PGPR promotes soil fertility and nutrient uptake by plants (*2*). Plant root exudates contain amino acids (*12*), organic acids (*13*) and sugars (*2*) that serve as nutrients for PGPR, and therefore are sensed by bacteria as attractants. Previous studies showed that mutation of the gene encoding the central chemotaxis regulatory protein CheA in *P. fluorescens* WCS365 resulted in less efficient colonization of tomato roots in comparison to the wild-type strain (*14*). Furthermore, a hyper-motile mutant of *P. fluorescens* F113 was shown to be a more efficient root-tip colonizer and to have a more significant effect in biological control of plant pathogenic fungi in comparison to the wild-type strain (*15*). Therefore, chemotaxis towards nutrients is thought to play a crucial role in effective root colonization by *P. fluorescens*.

Methyl-accepting chemotaxis proteins (MCPs) are membrane-embedded receptors that mediate chemotaxis

by recognizing chemical signal molecules (*16*). The binding of these molecules to the periplasmic sensing domains of MCPs initiates a chemotactic signalling cascade (*16*). The genome of *P. fluorescens* Pf0-1 encodes genes for 37 MCPs. Information on the ligands recognized by these receptors is limited. Three MCPs have been identified as chemotactic transducers of amino acids (CtaA, CtaB and CtaC) – receptors that recognize naturally-occurring amino acids (*17*). MCPs Pfl01_3768, Pfl_0728 and Pfl01_0728 were reported to recognize *L*-malate, succinate and fumarate (*18*). The metabolism of the aromatic compound 2-nitrobenzoate was shown to involve the chemoreceptor for 2-nitrobenzoate NbaY (*19*).

CtaA has a very broad ligand specificity and recognizes 16 different amino acids (*17*). The structural basis behind ligand recognition and the mechanism of signalling in response of ligand binding to CtaA remains unknown. A BLAST search against the known structures available in the Protein Data Bank (PDB) revealed that the periplasmic sensing domain of CtaA (CtaA^{peri}) has 30%, 24%, and 20% sequence identity with *V. cholerae* chemoreceptor MCP37 (PDB code 5AVE (*20*)), *Methanosarcina mazei* histidine kinase (PDB code 3li8, (*21*)) and *Campylobacter jejuni* chemoreceptor Tlp3 (PDB code 4xmr (*22*)), respectively. The periplasmic sensing domain of an amino acid chemotaxis receptor PctA from *Pseudomonas aeruginosa* that has 65% amino acid sequence identity with CtaA^{peri} (*17*) was crystallized in 2013 (*23*), but no report of the structure followed. The Pfam analysis (*24*) using the primary sequence of CtaA^{peri} revealed the presence of a Cache (*ca*lcium channels and *che*motaxis receptors) motif (residues 107-185) (*25*), which suggests that CtaA^{peri} belongs to the family of receptor proteins with two Per-Arnt-Sim (PAS) sensing domains. Recently, we have reported the crystal structure of the periplasmic sensing domain of *C. jejuni* transducer-like protein 3 (Tlp3) harboring two PAS domains. Tlp3 recognizes its ligand isoleucine directly, *via* its membrane-distal PAS domain (*22*). The structural analysis of Tlp3 and structure-guided sequence alignments revealed that receptors for amino acids, that have a tandem-PAS sensing domain that recognizes the ligand directly, contain a conserved consensus motif DXXX(R/K)CWYXXA (*22*). We note that CtaA^{peri} contains this motif and is therefore likely to bind at least some of its amino acid ligands directly. To investigate the structural basis of how CtaA recognizes its signal molecules and transduces the signal across the membrane, we have initiated structural studies on recombinant CtaA^{peri}. Here, we report its cloning, purification, co-crystallization with one of its putative ligands (serine) and initial X-ray crystallographic analysis.

2. Materials and Methods

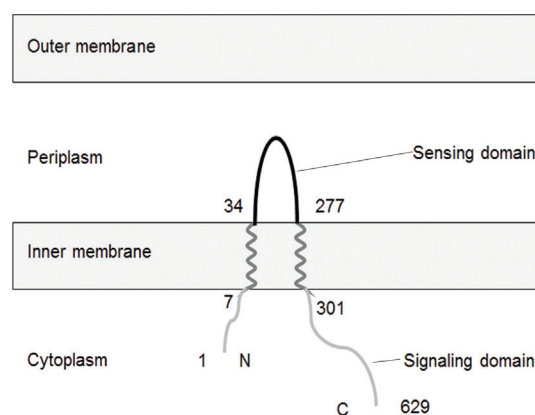### 2.1. *Gene cloning and overexpression*

Figure 1. The predicted membrane topology of *P. fluorescens* CtaA and the boundaries (amino acid residue numbers) of the periplasmic sensory domain CtaA^{peri} characterized in this study.

The two transmembrane helices of CtaA from *P. fluorescens* Pf0-1 (GenBank: ABA76168.1) have been predicted to comprise residues 7-33 and 278-301 by the TMHMM sever v.2.0 (*http://www.cbs.dtu.dk/services/TMHMM-2.0/*) (*26*) (Figure 1). The sequence for the periplasmic sensing domain (CtaA^{peri}, residues 34-277) was codon-optimized for expression in *Escherichia coli* and synthesized and ligated into the expression vector pET151/D-TOPO (Invitrogen) by GenScript. The protein construct had an N-terminal His$_6$-tag separated from the CtaA^{peri} coding sequence by the linker GKPIPNPLLGLDSTENLYFQ↓GIDPFT containing a Tobacco Etch Virus (TEV) protease cleavage site (underlined). The *E. coli* BL21 (DE3) cells (Novagen) were transformed with the expression vector, grown at 310 K in Luria Bertani broth supplemented with 50 mg/mL ampicillin to OD$_{600}$ of 0.6, and then protein expression was induced with 0.5 mM isopropyl-b-D-1-thiogalactopyranoside (Thermo Scientific) for 3.5 h at 310 K. The cells were harvested by centrifugation at 6,000 g for 15 min at 277 K.

2.2. *Purification*

The cells were resuspended in 20 mM Tris-HCl buffer pH 8.0 and 200 mM NaCl, lysed using sonication and centrifuged at 12,000 g for 30 min at 277 K. NaCl and imidazole were then added to the supernatant to final concentrations of 500 and 15 mM, respectively, and the sample was loaded onto a 5 mL HiTrap Chelating HP column (GE Healthcare) pre-washed with buffer A (20 mM Tris-HCl pH 8.0, 500 mM NaCl, 15 mM imidazole). The protein was eluted with buffer A, supplemented with 500 mM imidazole, after the column was washed with 20 column volumes of buffer A containing 20 mM imidazole. The N-terminal tag was cleaved with His$_6$-TEV protease overnight at 277 K whilst dialyzing the sample against buffer B [50 mM Tris-HCl pH 8.0, 2 mM dithiothreitol, 200 mM NaCl, 1% (*v/v*) glycerol]. NaCl
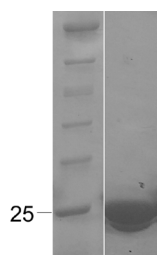
Figure 2. Coomassie Blue-stained 15% SDS-PAGE gel of recombinant CtaA^peri. The left lane contains molecular-weight marker (labelled in kDa).

and imidazole were then added to the sample to final concentrations of 500 and 15 mM, respectively, and the TEV protease and the uncleaved protein were removed on a HiTrap Chelating HP column. The flowthrough was concentrated to 2 mL in an Amicon Ultracel 10 kDa cutoff concentrator and purified further by passing through a Superdex 200 HiLoad 26/60 gel-filtration column (GE Healthcare) equilibrated with buffer C (10 mM Tris-HCl pH 8.0, 200 mM NaCl). Protein concentration was determined using the Bradford assay (*27*). The protein purity was estimated to be greater than 98% (Figure 2).

2.3. *Crystallization*

Prior to crystallization, the protein sample was concentrated to 10 mg/mL, mixed with serine solution (final concentration 2 mM), centrifuged for 20 min at 13,000 g and transferred into a clean tube. Initial crystallization screening was performed by the vapour-diffusion method in the hanging-drop format using an automated Phoenix crystallization robot (Art Robbins instruments) and Crystal Screen HT, Index Screen HT and PEG/Ion Screen HT (Hampton Research). The initial crystallization droplets comprised 100 nL protein solution mixed with 100 nL of the reservoir solution and equilibrated against 50 μL of the reservoir solution in a 96-well Art Robbins Crystalmation Intelli-Plate (Hampton Research). After one day, crystals appeared from condition No. 6 of Index Screen HT, which contained 2.0 M ammonium sulfate and 0.1 M Tris-HCl pH 8.5. This condition was further optimized to improve the crystals quality, yielding an optimal crystallization reservoir solution consisting of 2.0 M ammonium sulfate and 0.1 M Tris-HCl pH 8.0 (Figure 3).

2.4. *Data collection and processing*

Prior to data collection, crystals were transferred from the crystallization drop into a cryoprotectant solution containing 0.1 M Tris-HCl pH 8.0, 2.2 M ammonium sulfate, 2 mM serine and 30% (*v/v*) glycerol, and flash-cooled by plunging in liquid nitrogen. A complete X-ray diffraction data set was collected from a single crystal to 1.9 Å resolution using an ADSC Quantum 210r
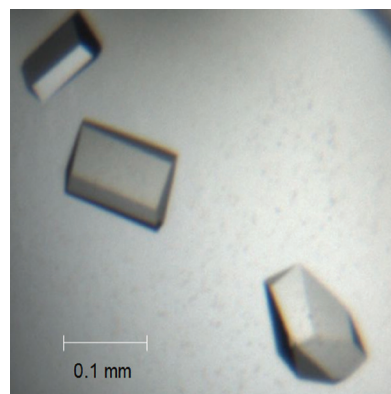

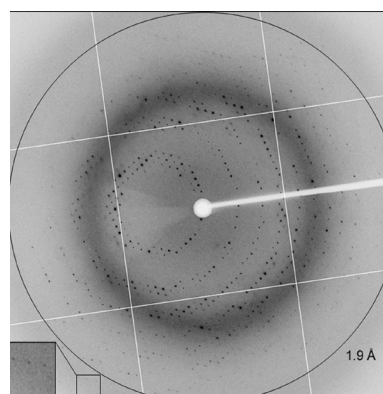**Figure 3. Crystals of a putative CtaA^peri complex with serine.**

Figure 4. A representative 0.5° oscillation image of the data collected using an ADSC Quantum 210r CCD detector on the MX1 station of the Australian Synchrotron, Victoria, Australia. A magnified rectangle shows diffraction spots beyond 1.9 Å resolution.

CCD detector on the MX1 beamline of the Australian Synchrotron (AS) (Figure 4). A total of 90 images were collected using a 0.5° oscillation width. The data were processed and scaled using *iMosflm* (*28*) and *AIMLESS* (*29*) from the *CCP4* suite (*30*). The statistics of data collection and processing are summarized in Table 1.

3. Results and Discussion

Recombinant *P. fluorescens* CtaA^peri was over-expressed in *E. coli* BL21 (DE3) harboring pET151/D-TOPO plasmid upon induction of T7 polymerase. The protein was purified to >98% electrophoretic homogeneity based on Coomassie Blue staining of SDS-PAGE gels (Figure 2). It consists of amino-acid residues 34-277 of CtaA with six additional residues at the N terminus originating from the TEV cleavage site (GIDPFT). The protein migrated on SDS-PAGE with an apparent molecular weight of 25 kDa, which is in agreement with the value calculated from the amino acid sequence (27 kDa). It eluted as a single peak during size-exclusion chromatography (SEC). Estimation of its molecular weight from the mobility on the SEC column calibrated with reference to the mobility of globular proteins of

Table 1. Data collection and processing. Values for the outer shell are given in parentheses

Diffraction source	MX1 beamline, Australian Synchrotron
Wavelength (Å)	1.0
Temperature (K)	100
Detector	ADSC Quantum 210r CCD
Rotation range per image (°)	0.5
Total rotation range (°)	90
Exposure time per image (s)	1
Space group	$I222$ or $I2_12_12_1$
a, b, c (Å)	67.2, 76.0, 113.3
α, β, γ (°)	90, 90, 90
Mosaicity (°)	0.8
Resolution range (Å)	33.8-1.9
Total No. of reflections	79149 (5083)
No. of unique reflections	21256 (1353)
Completeness (%)	92.3 (94.0)
Redundancy	3.7 (3.8)
$<I/\sigma(I)>$	12.7 (2.5)
$R_{\text{r.i.m.}}$	0.029 (0.220)
Overall B factor from Wilson plot (Å2)	26.3

a known mass gave the value of approximately 23 kDa, which suggested that *P. fluorescens* CtaA$^{\text{peri}}$ is monomeric in solution under the tested conditions.

An X-ray diffraction data set was collected for a cryo-cooled crystal of CtaA$^{\text{peri}}$ grown in the presence of serine to 1.9 Å using the AS facility (Figure 4). Data analysis by the autoindexing routine in *iMosflm* was consistent with a body-centred orthorhombic crystal system ($I222$ or $I2_12_12_1$), with unit cell parameters a = 67.2, b = 76.0, c = 113.3 Å. The average $I/\sigma(I)$ value was 12.7 for all reflections (resolution range 33.8-1.9 Å) and 2.5 in the highest resolution shell (1.94-1.90 Å). Data processing gave an R_{merge} of 0.051 for intensities (0.346 in the resolution shell 1.94-1.90 Å) and these data were 92% complete (94% completeness in the highest resolution shell).

The calculated Matthews coefficient (*31*) for one subunit of CtaA$^{\text{peri}}$ was 2.64 Å^3 Da^{-1}, which suggests that the asymmetric unit is highly likely to contain one protein molecule. The corresponding solvent content is approximately 53%. Molecular replacement approaches with the structures of the sensing domains of *V. cholerae* MCP37, *M. mazei* histidine kinase or *C. jejuni* Tlp3 did not yield a reliable solution. A search for heavy-atom derivatives with the aim to solve the structure using multiple isomorphous replacement and/or multi-wavelength anomalous dispersion methods is in progress. Structural analysis of the CtaA would be an important step towards our understanding of how CtaA senses its environmental signals and communicates inside the cell *via* the membrane.

Acknowledgements

References

1. Vacheron J, Desbrosses G, Bouffaud M-L, Touraine B, Prigent-Combaret C. Plant growth-promoting rhizobacteria and root system functioning. Front Plant Sci. 2013; 17:356.
2. Lugtenberg B, Kamilova F. Plant-growth-promoting rhizobacteria. Annu Rev Microbiol. 2009; 63:541-556.
3. Couillerot O, Prigent-Combaret C, Caballero-Mellado J, Moënne-Loccoz Y. *Pseudomonas fluorescens* and closely-related fluorescent pseudomonads as biocontrol agents of soil-borne phytopathogens. Lett Appl Microbiol. 2009; 48:505-512.
4. Haas D, Défago G. Biological control of soil-borne pathogens by fluorescent pseudomonads. Nat Rev Microbiol. 2005; 3:307-319.
5. O'sullivan DJ, O'Gara F. Traits of fluorescent *Pseudomonas* spp. involved in suppression of plant root pathogens. Microbiol Rev. 1992; 56:662-676.
6. Van Loon L, Bakker P, Pieterse C. Systemic resistance induced by rhizosphere bacteria. Annu Rev Phytopathol. 1998; 36:453-483.
7. Beltrametti F, Marconi AM, Bestetti G, Colombo C, Galli E, Ruzzi M, Zennaro E. Sequencing and functional analysis of styrene catabolism genes from *Pseudomonas fluorescens* ST. Appl Environ Microbiol. 1997; 63:2232-2239.
8. Pak JW, Knoke KL, Noguera DR, Fox BG, Chambliss GH. Transformation of 2, 4, 6-Trinitrotoluene by purified xenobiotic reductase B from *Pseudomonas fluorescensI*-C. Appl Environ Microbiol. 2000; 66:4742-4750.
9. Caldini G, Cenci G, Manenti R, Morozzi G. The ability of an environmental isolate of *Pseudomonas fluorescens* to utilize chrysene and other four-ring polynuclear aromatic hydrocarbons. Appl Microbiol Biotechnol. 1995; 44:225-229.
10. Wei B, Huang T, Dalwadi H, Sutton CL, Bruckner D, Braun J. *Pseudomonas fluorescens* encodes the Crohn's disease-associated I2 sequence and T-cell superantigen. Infect Immun. 2002; 70:6567-6575.
11. Scales BS, Dickson RP, LiPuma JJ, Huffnagle GB. Microbiology, genomics, and clinical significance of the *Pseudomonas fluorescens* species complex, an unappreciated colonizer of humans. Clin Microbiol Rev. 2014; 27:927-948.
12. Simons M, Permentier HP, de Weger LA, Wijffelman CA, Lugtenberg BJ. Amino acid synthesis is necessary for tomato root colonization by *Pseudomonas fluorescens* strain WCS365. Mol Plant Microbe Interact. 1997; 10:102-106.
13. Kamilova F, Kravchenko LV, Shaposhnikov AI, Azarova T, Makarova N, Lugtenberg B. Organic acids, sugars, and L-tryptophane in exudates of vegetables growing on stonewool and their effects on activities of rhizosphere bacteria. Mol Plant Microbe Interact. 2006; 19:250-256.
14. de Weert S, Vermeiren H, Mulders IH, Kuiper I, Hendrickx N, Bloemberg GV, Vanderleyden J, De Mot R, Lugtenberg BJ. Flagella-driven chemotaxis towards exudate components is an important trait for tomato root

colonization by *Pseudomonas fluorescens*. Mol Plant Microbe Interact. 2002; 15:1173-1180.

15. Barahona E, Navazo A, Martínez-Granero F, Zea-Bonilla T, Pérez-Jiménez RM, Martín M, Rivilla R. *Pseudomonas fluorescens* F113 mutant with enhanced competitive colonization ability and improved biocontrol activity against fungal root pathogens. Appl Environ Microbiol. 2011; 77:5412-5419.

16. Kato J, Kim H-E, Takiguchi N, Kuroda A, Ohtake H. *Pseudomonas aeruginosa* as a model microorganism for investigation of chemotactic behaviors in ecosystem. J Biosci Bioeng. 2008; 106:1-7.

17. Oku S, Komatsu A, Tajima T, Nakashimada Y, Kato J. Identification of chemotaxis sensory proteins for amino acids in *Pseudomonas fluorescens* Pf0-1 and their involvement in chemotaxis to tomato root exudate and root colonization. Microbes Environ. 2012; 27:462-469.

18. Oku S, Komatsu A, Nakashimada Y, Tajima T, Kato J. Identification of *Pseudomonas fluorescens* chemotaxis sensory proteins for malate, succinate, and fumarate, and their involvement in root colonization. Microbes Environ. 2014; 29:413-419.

19. Iwaki H, Muraki T, Ishihara S, Hasegawa Y, Rankin KN, Sulea T, Boyd J, Lau PC. Characterization of a pseudomonad 2-nitrobenzoate nitroreductase and its catabolic pathway-associated 2-hydroxylaminobenzoate mutase and a chemoreceptor involved in 2-nitrobenzoate chemotaxis. J Bacteriol. 2007; 189:3502-3514.

20. Nishiyama S, Takahashi Y, Yamamoto K, Suzuki D, Itoh Y, Sumita K, Uchida Y, Homma M, Imada K, Kawagishi I. Identification of a *Vibrio cholerae* chemoreceptor that senses taurine and amino acids as attractants. Sci Rep. 2016; 6:20866.

21. Zhang Z, Hendrickson WA. Structural characterization of the predominant family of histidine kinase sensor domains. J Mol Biol. 2010; 400:335-353.

22. Liu YC, Machuca MA, Beckham SA, Gunzburg MJ, Roujeinikova A. Structural basis for amino-acid recognition and transmembrane signalling by tandem Per-Arnt-Sim (tandem PAS) chemoreceptor sensory domains.

Acta Cryst D. 2015; 71:2127-2136.

23. Rico-Jiménez M, Muñoz-Martínez F, Krell T, Gavira JA, Pineda-Molina E. Purification, crystallization and preliminary crystallographic analysis of the ligand-binding regions of the PctA and PctB chemoreceptors from *Pseudomonas aeruginosa* in complex with amino acids. Acta Cryst F. 2013; 69:1431-1435.

24. Finn RD, Bateman A, Clements J, Coggill P, Eberhardt RY, Eddy SR, Heger A, Hetherington K, Holm L, Mistry J. Pfam: The protein families database. Nucleic Acids Res. 2014:gkt1223.

25. Anantharaman V, Aravind L. The CHASE domain: A predicted ligand-binding module in plant cytokinin receptors and other eukaryotic and bacterial receptors. Trends Biochem Sci. 2001; 26:579-582.

26. Krogh A, Larsson B, Von Heijne G, Sonnhammer EL. Predicting transmembrane protein topology with a hidden Markov model: Application to complete genomes. J Mol Biol. 2001; 305:567-580.

27. Bradford MM. A rapid and sensitive method for the quantitation of microgram quantities of protein utilizing the principle of protein-dye binding. Anal Biochem. 1976; 72:248-254.

28. Battye TGG, Kontogiannis L, Johnson O, Powell HR, Leslie AG. iMOSFLM: A new graphical interface for diffraction-image processing with MOSFLM. Acta Cryst D. 2011; 67:271-281.

29. Evans PR, Murshudov GN. How good are my data and what is the resolution? Acta Cryst D. 2013; 69:1204-1214.

30. Winn MD, Ballard CC, Cowtan KD, Dodson EJ, Emsley P, Evans PR, Keegan RM, Krissinel EB, Leslie AG, McCoy A. Overview of the CCP4 suite and current developments. Acta Cryst D. 2011; 67:235-242.

31. Matthews B. In: H. Neurath, Hill RL, editors. X-ray Structure of Proteins. 3. 3rd ed. Academic Press, New York, USA 1977. pp. 468-477.